Ahsanullah University
of Science and Technology

Characteristic Analysis of Polarization and Dispersion Properties of PANDA Fiber Using Finite Element Methods

Sanjib Das[1], Anindya Jyoti Dutta[1], Nurmohammed Patwary[1],
M. Shah Alam[1]

Abstract : One possible structure of a PANDA fiber is proposed and the effects of hydraulic stress on the propagation properties are studied in this work. The proposed PANDA fiber can withstand up to 1500MPa external hydraulic stress while maintaining the fundamental mode of propagation. Effects of hydraulic pressure on several propagation properties such as birefringence, beat length, effective index, dispersion, cutoff wavelength, and bandwidth are shown in this paper.

Keywords : Birefringence, dispersion, finite element method, hydraulic stress effects, polarization properties, stress analysis

1. Introduction

The polarization state of light is of considerable importance in both coherent optical communication and fiber optic systems. Moreover, interference and delay differences between orthogonally polarized modes may cause polarization modal noise and polarization mode dispersion in birefringent fiber. Hence, there are several reasons why it may be desirable to use fiber that will permit light to pass through whilst retaining its state of polarization [1]-[2]. Polarization maintaining and absorption reducing fiber, which is called PANDA fiber, is one of the most commonly used high birefringent polarization maintaining fibers (PMFs) [1]-[9]. It has been shown that polarimetric and interferometric fiber-optic sensing devices composed of highly birefringent (HB) fibers are very effective for precisely registering a variety of measurands including temperature, strain and hydraulic stress [3]. The potential advantages of using fibers of these types are immunity to electromagnetic interference, suitability for adverse environments and effectiveness even in very high hydraulic stress condition [3]. The objective of this work is to analyze the effect of external hydraulic stress on fiber geometry and fiber characteristics and determine the maximum amount of stress it can withstand.

Modal birefringence is an important parameter, used to describe the polarization maintaining capability of single mode PMFs [10]. These fibers with circular symmetry about the core axis allow the propagation of two nearly degenerate modes with orthogonal polarizations. They are therefore bimodal supporting HE_{11}^{x} and HE_{11}^{y} modes, where the principle axes x and y are determined by the symmetry elements of the fiber cross section [1]-[4], [7]-[9]. Thus, the fiber behaves as a birefringent medium due to the difference in refractive indices between two orthogonally polarized modes.

Because of the stress applying zones (SAZs) and the cladding have different thermal expansion coefficients, it is anticipated that the birefringence in any PMF is sensitive to temperature variations [4], [7]-[9]. Different birefringent fibers and their stress dependent properties can be found in the literature [11]-[21]. In this study, it is found that birefringence is sensitive to the change of hydraulic pressure. Here, the effect of hydraulic pressure on beat length, which describes the length required for the polarization to rotate 360 degrees, dispersion, effective index, and cutoff wavelength are also discussed. The authors' intention is to propose a structure of PMF, which can be effectively used in under water communication, where external pressure is rather high.

2. Structural and Physical Properties

Fig. 1 shows the cross section of the PANDA fiber simulated in this work. Three different types of glass materials are used for three different regions of the fiber. These are LITHOTEC-CAF2 for cladding, N-FK51A for core and LITHOSIL-Q for SAZs. Different structural and physical parameters of the fiber are shown in Table 1. Pitch (Γ), the distance between the centers of core and SAZ is 24.70 µm. The different refractive indices at different wavelengths are obtained using Sellmeier equation [1]-[2]

$$n(\lambda) = 1 + \frac{B_1\lambda^2}{\lambda^2 - \lambda_1} + \frac{B_2\lambda^2}{\lambda^2 - \lambda_2} + \frac{B_3\lambda^2}{\lambda^2 - \lambda_3} \tag{1}$$

Here B_1, B_2, B_3, λ_1, λ_2 and λ_3 are the experimentally determined Sellmeier coefficients, and n is the refractive index at

[1] *Department of Electrical and Electronic Engineering, Bangladesh University of Engineering and Technology (BUET), Dhaka-1000, Bangladesh*

wavelength λ. Table 2 shows the corresponding Sellmeier coefficients for three different materials of the fiber.
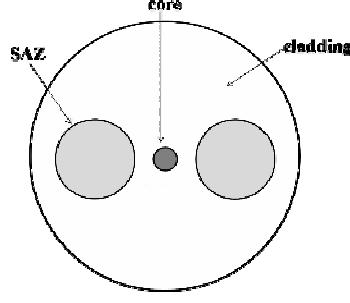

Fig. 1. The cross section of the PANDA fiber.

Table 1: Structural and Physical Parameters of the Fiber.

Fiber region	Core	Cladding	SAZ
Radius (µm)	4.05	62.5	19.5
Glass	N-FK51A	LITHOTEC-CAF2	LITHOSIL-Q
Refractive index (at λ = 1.3µm)	1.47774	1.42722	1.44690
Young´s modulus, E (N/m^2)	73×10^9	76×10^9	72×10^9
Poisson ratio, ν	0.302	0.26	0.17
Thermal expansion coefficient, α (k^{-1})	12.74	18.41	0.5

Table 2: Sellmeier Coefficients of Fiber Materials.

Glass materials	N-FK51A	LITHOTEC-CAF2	LITHOSIL-Q
B_1	0.971247817	0.617617011	0.67071081
λ_1 (µm^2)	0.00472301995	0.00275381936	0.00449192312
B_2	0.216901417	0.421117656	0.433322857
λ_2 (µm^2)	0.0153575612	0.0105900875	0.0132812976
B_3	0.904651666	3.79711183	0.877379057
λ_3 (µm^2)	168.68133	1182.67444	95.8899878

3. Methodology

To obtain the polarization properties of the optical fiber under thermal and external stress the finite element method (FEM) [22] is used in this work. First the stress analysis is carried out using plane strain approximation, where the stress in the longitudinal direction is neglected, and the stress-optic effect is incorporated to find the change in refractive indices of fiber materials. Then with the new indices, optical analysis is carried out using a vector FEM to obtain the modal propagation properties. The fiber is assumed to be uniform in longitudinal direction and the cross section of the fiber is divided into many small Lagrange type triangular elements during the analysis.

3.1 Stress Analysis

To include the effect of thermal stress and external stress on propagation properties of the fibers, the stress analysis is carried out using the plane strain approximation [7]. The system formulation is carried out for unknown displacements due to strain caused by the stresses over the cross section of the fiber. After solving the system for unknown displacements, one can easily find the stresses in different directions σ_x, σ_y, and σ_z and find the anisotropic change in refractive indices due to stress-optic effect. These anisotropic changes are calculated using stresses and stress-optic coefficients K_1 and K_2 as

$$\Delta n_{x0} = n_x - n_0 = -K_2\sigma_x - K_1(\sigma_y + \sigma_z)$$
$$\Delta n_{y0} = n_y - n_0 = -K_2\sigma_y - K_1(\sigma_z + \sigma_x)$$
$$\Delta n_{z0} = n_z - n_0 = -K_2\sigma_z - K_1(\sigma_x + \sigma_y)$$

(2)

Here n_0 is the isotropic refractive index of the unstressed fiber material, and the n_x, n_y, and n_z are the principal diagonal components of anisotropic refractive index tensor when the stress-optic effect is incorporated. The refractive index of unstressed fiber material at different wavelengths may be obtained using Sellmeier equation (1).

3.2 Optical Analysis
To carry out the optical analysis, the resulting anisotropic refractive indices as calculated by equation (2) are used. The modal analysis is carried out assuming that the fiber is uniform in z-direction and the wave propagates along the z-direction with time and phase variation of $e^{j\omega t}$ and $e^{-j\beta z}$, respectively. Here ω is the angular frequency and β is the propagation constant. An eigenvalue equation in terms of the magnetic field can be obtained from the Helmholtz equation

$$\nabla \times ([n]^{-2} \nabla \times \mathbf{H}) - k_0^2 \mathbf{H} = \mathbf{0} \qquad (3)$$

and is solved for modal effective index, $n_{eff} = \beta/k_0$, as the eigenvalue. For optical analysis using [22], however, a module based on the perpendicular hybrid mode wave using transversal fields is used for finding the modal solutions. Once, equation (3) is solved, the effective indices, mode field distribution, and power distribution over the cross section of the fiber can be readily obtained for further processing to obtain various fiber properties.

4. Results and Discussions
While performing the thermal stress analysis, stress distribution along the cross section of the fiber is observed as the Von Mises Stress (N/m^2). Fig. 2 shows the distribution of displacement vectors in different regions of the fiber caused by the applied hydraulic and thermal stress on the fiber. It is obvious that displacement vectors are greater at the edge of cladding and the length of arrows gradually decreases towards the center of the core. At the center of the core, the displacement is almost negligible. It implies that at the outer cladding surface, the stress would be highest. The core would experience the least stress. Fig. 3 shows the normalized power distribution of fundamental mode of propagation, where it can be observed that the maximum power is confined in the core region as expected. The optical analysis is carried out with the new refractive indices after the stress analysis.
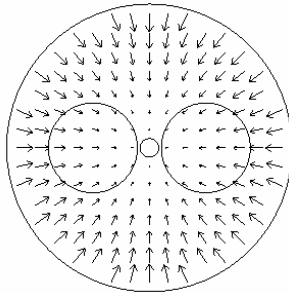

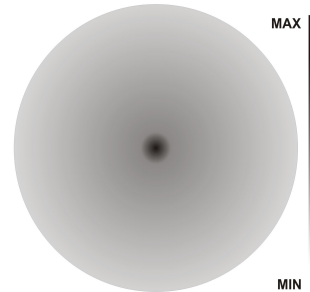Fig. 2. Distribution of displacement vector.   Fig. 3. Power distribution over   the cross section.

Now, to observe the effect of external stress on the fiber properties, three hydraulic stress values of 0, 0.5 GPa and 1.0 GPa are applied on the fiber, separately, on the fiber when the pitch is 24.7µm. The effect of wavelength variation on birefringence is shown in Fig. 4. It is obvious that with no hydraulic stress (only thermal stress), birefringence varies from a value near 4×10^{-3} to 6×10^{-3} for wavelength variation in visible light range. For the stress of 0.5 GPa, the value is higher than 6×10^{-3}, but for higher values of hydraulic stress, it decreases. Another worth mentioning fact is the non-varying nature of birefringence with the change of wavelength at a particular hydraulic stress.

Fig. 5 shows the change in beat length, which increases with the increase in applied hydraulic stress but with no hydraulic stress, the variation is random. For all cases, the tendency of change is upward with the increase in optical wavelength. A different scenario is observed for effective index, where it decreases with the increase in wavelength. Fig. 6 shows that effective index at a particular wavelength increases with the increase in applied hydraulic stress.
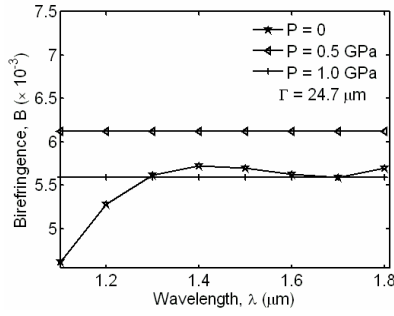
Fig. 4. Birefringence variation
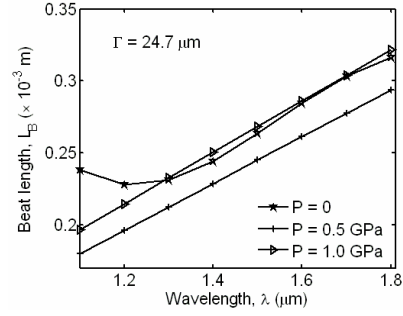with wavelength.

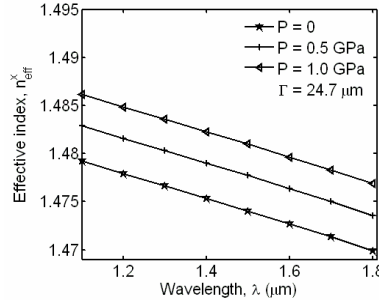
Fig. 5. Beat length variation
with wavelength.

Fig. 6. Effective index variation with wavelength.

Dispersion is another important parameter that must be taken into account for any optical fiber communication link. It is the broadening of light pulses, which is a critical factor limiting the quality of signal transmission medium [1]-[2]. The effects of hydraulic stress on dispersion with the change in wavelength are shown in Fig. 7. It can be seen that dispersion increases with the increase in wavelength but does not have a regular pattern. It is found that dispersion without hydraulic pressure and with a smaller vaue of 0.5 GPa are almost equal in magnitude. But at a higher value of 1.0 GPa, dispersion changes significantly. The change is very much significant at higher wavelength, which means that after a certain amount of stress, efficiency of communication decreases. Polarization mode dispersion (PMD) is another type of dispersion, which plays an important role in determining the performance of any optical fiber communication link. It can be defined as the broadening of the input pulse due to a phase delay between input polarization states. Actually, birefringence causes one polarization mode to travel faster than the other, resulting in a difference in the propagation time called the differential group delay, which in turn, causes PMD [2]. PMD has a proportional relationship with group birefringence and inverse relationship with the velocity of light. Fig. 8 depicts the effect of hydraulic stress on PMD. The PMD increases with the increase in wavelength when there is no hydraulic stress on the fiber. This variation is significant at lower wavelength but at higher wavelengths the variation is very small and insignificant. However, under hydraulic stress, the PMD is almost constant over the wavelength band considered here.
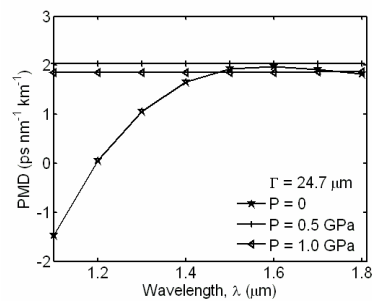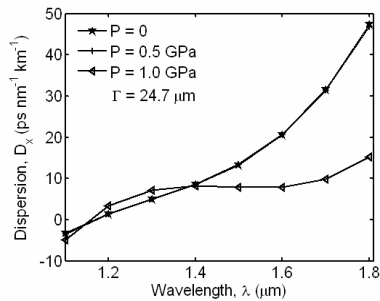

Fig. 7. Dispersion variation with wavelength.   Fig. 8. PMD variation with
wavelength.

Finally, the effects of hydraulic stress on several other factors, such as cutoff wavelength, bandwidth and maximum electric field are analyzed and discussed. Fig. 9 shows the effect of hydraulic stress on cutoff wavelength and bandwidth. Cut-

off wavelength can be defined as the maximum wavelength that will propagate in an optical fiber or waveguide. It can be seen from the figure that cutoff wavelength increases with the increase in pressure, implying that with the increased stress, the information carrying possibility would reduce. So the lowest wavelength that would support the fundamental mode of propagation would shift towards higher value with stress. As for bandwidth, it can be seen that it is also increasing with the increase in pressure. Next, the effect of hydraulic stress on maximum electric field inside the fiber is shown in Fig. 10. It is observed that for both x and y polarized light, the maximum electric field intensity decreases with the increase in hydraulic stress.
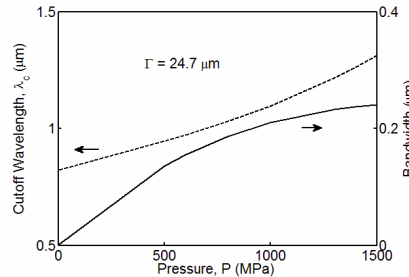

Fig. 9. Variation of cutoff wavelength and bandwidth with pressure.
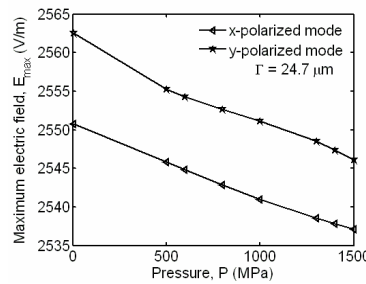

Fig. 10. Variation in maximum electric field with pressure

Now, Fig. 11 shows a comparative analysis of normalized power flow for three distinct cases, i.e., fiber without stress, under only thermal stress, and under hydraulic stress. It can be seen that the power density is larger when there is no stress on the fiber. However, it decreases when there is thermal stress on the fiber. This further reduces, when additional hydraulic stress is present. Table 3 shows normalized power and mode field diameter at different stress conditions. The table shows that mode field diameter is minimal when no stress was applied and highest when only thermal stress was applied on fiber.
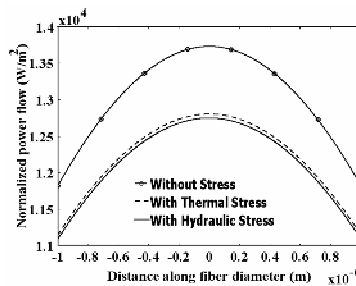

Fig. 11. Comparison of normalized power flow

Table 3 : Comparison of Normalized Power Flow.

Cases	Normalized power (W/m^2)	Mode field diameter (m)
Without stress	1.373×10^4	4.96×10^{-6}
With thermal stress	1.281×10^4	5.12×10^{-6}
With hydraulic stress	1.275×10^4	5.102×10^{-6}

5. Conclusion

In this work, a structure of PANDA fiber is proposed, and is simulated to obtain the propagation properties when the fiber is under external hydraulic pressure. It was found that up to almost 1500MPa, the fundamental mode power was confined at core with sufficiently high birefringence. Beat length increases with the applied pressure which is a disadvantage for under water communication but this property can be used for pressure sensor applications. Under stress, the dispersion of PANDA fiber shows flattened nature while the PMD remains constant over a wide range of wavelength. The cut-off wavelength and the bandwidth of this fiber increase with the increase in external pressure. The significant changes in propagation properties indicate that careful consideration is needed during application of such birefringent fibers. More complex structures may also be analyzed in future.

References

1. J. M. Senior, Optical Fiber Communication: Principle and Practice, 2nd ed., Prentice-Hall International Ltd., 1992.
2. G. P. Agrawal, Fiber-Optic Communication Systems, 3rd edition, John Wiley & Sons, Inc., 2005.
3. W. J. Bock, W. Urbanczyk, J. Wojcik, and M. Beaulieu, "White-light interferometric fiber-optic pressure sensor," IEEE Trans. Instrum. Meas., vol. 44, pp. 70b-708, 1995.
4. V. Ramaswamy, R. H. Stolen, M. Divino, and W. Pleibel, "Birefringence in elliptically clad borosilicate single-mode fibers,'' Appl. Opt., vol. 18, pp. 4080-4084, 1979.
5. D. Chowdhury and D. Wilcox, "Comparison between optical fiber birefringence induced by stress anisotropy and geometric deformation," J. Select. Topics Quantum Electron, vol. 6, pp. 227-232, 2000.
6. W. J. Bock, A. W. Domanski, and T. R. Wolinski, "Influence of high hydrostatic pressure on beat length in highly birefringent single-mode bow tie fibers," Appl. Opt., vol. 29, no. 24, pp. 3484-3488, Aug. 1990.
7. K. Okamoto, Fundamentals of Optical Waveguides, Academic Press, 2000.
8. Y. Liu, B. M. A. Rahman, and K. T. V. Grattan, "Thermal-stress-induced birefringence in bow-tie optical fibers," Appl. Opt., vol. 33, no. 24, pp. 5611-5616, Aug. 1994.
9. Y. Liu, B. M. A. Rahman, and K. T. V. Grattan, "Analysis of the birefringence properties of optical fibers made by a perform deformation technique," J. Lightw. Technol., vol. 13, no. 2, pp. 142-147, Feb. 1995.
10. M.-J. Li, X. Chen, D. A. Nolan, G. E. Berkey, J. Wang, W. A. Wood, and L. A. Zenteno, "High bandwidth single polarization fiber with elliptical central air hole," J. Lightw. Technol., vol. 23, no. 11, pp. 3454-3460, Nov. 2005.
11. H. M. Xie, Ph. Dabkiewicz, and R. Ulrich, "Side-hole fiber for fiber-optic pressure sensing," Opt. Lett., vol. 11, no. 5, pp. 333-335, May 1986.
12. J. R. Clowes, S. Syngellakis, and M. N. Zervas, "Pressure sensitivity of side-hole optical fiber sensors," IEEE Photon. Technol. Lett., vol. 10, no. 6, pp. 857-859, June 1998.
13. W. J. Bock and A. W. Domanski, "High hydrostatic pressure effects in highly birefringent optical fibers," J. Lightw. Technol., vol. 7, no. 8, pp. 1279-1283, Aug. 1989.
14. M. E. Lines, "Physical origin of the temperature dependence of chromatic dispersion in fused silica," J. Appl. Phys., vol. 73, no. 5, pp. 2075-2079, Mar. 1993.
15. K. S. Kim and M. E. Lines, "Temperature dependence of chromatic dispersion in dispersion-shifted fibers: experiment and analysis," J. Appl. Phys., vol. 73, no. 5, pp. 2069-2074, Mar. 1993.
16. R. Passy, A. L. Gama, N. Gisin, and J. P. v. d. Weid, "Pressure dependence of polarization mode dispersion in hibi fibers," J. Lightw. Technol., vol. 10, no. 11, pp. 1527-1531, Nov. 1992.
17. T. Schreiber, H. Schultz, O. Schmidt, F. Röser, J. Limpert, and A. Tünnermann, "Stress-induced birefringence in large-mode-area micro-structured optical fibers," Opt. Express, vol. 13, no. 10, May 2005.
18. A. Michie, J. Canning, K. Lyytikäinen, M. Åslund, and J. Digweed, "Temperature independent highly birefringent photonic crystal fibre," Opt. Express, vol. 12, no. 21, Oct. 2004.
19. M. Szpulak, T. Martynkien, and W. Urbanczyk, "Effects of hydrostatic pressure on phase and group modal birefringence in microstructured holey fibers," Applied Optics, vol. 43, no. 24, August 2004.
20. Z. Li, C. Wu, H. Dong, P. Shum, C. Y. Tian, and S. Zhao, "Stress distribution and induced birefringence analysis for pressure vector sensing based on single mode fibers," Opt. Express, vol. 16, no. 6, Mar. 2008.
21. X. Chen, M.-J. Li, J. Koh, and D. A. Nolan, "Wide band single polarization and polarization maintaining fibers using stress rods and air holes," Opt. Express, vol. 16, no. 16, pp. 12060-12068, 2008.
22. COMSOL Multiphysics, version 3.2, Sept. 2005.

---

[1] *Department of Electrical and Electronic Engineering, Bangladesh University of Engineering and Technology (BUET), Dhaka-1000, Bangladesh*